Grażyna Ryzińska[1]*, Roman Gieleta[2]

[1] Rzeszow University of Technology, al. Powstańców Warszawy 12, 35-959 Rzeszow, Poland
[2] Military University of Technology, ul. gen. Witolda Urbanowicza 2, 00-908 Warsaw, Poland
* Corresponding author. E-mail: grar@prz.edu.pl

EXPERIMENTAL STUDIES ON IMPACT OF CFRP TUBES STRUCTURE ON AMOUNT OF ABSORBED ENERGY UNDER DYNAMIC CONDITIONS

The aim of this work is to examine the effect of the layer configuration (lay-up) of carbon 3k/IMP503Z40 epoxy composite elements on the specific energy absorption (SEA) effect in the process of progressive crushing of composite tubes. Composite tubes made of Impregnatex Compositi prepreg with a dry areal weight of 160 g/m² plain weave and unidirectional prepreg (UD) 200 g/m² on an epoxy matrix were tested. The resin content in both prepregs was 47%. Using these two materials, tubes with different ratios of axial and hoop fibers, in two sizes with an inner diameter of 42 and 20 mm while maintaining a constant ratio of wall thickness to a diameter of 0.05 were made. The samples were unilaterally chamfered at the angle of 70°. Then, tests of progressive crushing of the samples under dynamic conditions by means of a drop tower and an additional initiator were performed. A new factor was introduced to describe the mass fraction of the axial fibers. SEA was calculated, which indicated that the higher the share of axial fibers, the greater the SEA for both types of samples and it was indicated that there may be a scale effect.

Keywords: CRFP, SEA, prepreg, dynamic conditions

BADANIA EKSPERYMENTALNE WPŁYWU STRUKTURY RUR CFRP NA ILOŚĆ POCHŁANIANEJ ENERGII W WARUNKACH DYNAMICZNYCH

Celem niniejszej pracy jest zbadanie wpływu konfiguracji warstw elementów kompozytowych włókno węglowe 3k/żywica epoksydowa IMP503Z40 na efekt pochłaniania energii (SEA) w procesie progresywnego niszczenia rur kompozytowych. Badano rury kompozytowe wykonane z preimpregnatu firmy Impregnatex Compositi o gramaturze suchej tkaniny 160 g/m² o splocie płóciennym oraz preimpregnatu jednokierunkowego (UD) 200 g/m² na osnowie epoksydowej. Zawartość żywicy w obu preimpregnatach wynosiła 47%. Wykorzystując te dwa materiały, wykonano rury o różnym stosunku ilości włókien osiowych do obwodowych, w dwóch rozmiarach o średnicy wewnętrznej 42 mm oraz o średnicy wewnętrznej 20 mm, zachowując stały stosunek grubości ścianki do średnicy wynoszący 0,05. Próbki jednostronnie fazowano pod kątem 70°. Następnie wykonano testy progresywnego niszczenia próbek w warunkach dynamicznych z zastosowaniem młota opadowego oraz dodatkowego elementu - inicjatora. Wprowadzono nowy współczynnik do opisu udziału masowego włókien osiowych. Obliczono wartości zaabsorbowanej energii (SEA), które wskazują, że im większy udział włókien osiowych, tym większa ilość zaabsorbowanej energii dla obu typów próbek, oraz wskazano na prawdopodobne występowanie efektu skali.

Słowa kluczowe: CRFP, SEA, preimpregnat, warunki dynamiczne

INTRODUCTION

Research shows that a properly designed composite material is able to absorb more energy per unit of mass than metal. Energy absorbing structures should be designed in such a way that during an accident this energy can be absorbed gradually in a controlled manner, and above all, be safe for passengers. The automotive, aerospace and railway industries are constantly looking for new solutions to produce increasingly lighter vehicles that simultaneously meet high safety standards. Composite products are already widely used in this area as structural elements, however, they also have a great potential as energy absorbing elements in a wide range of automotive and aviation products since they are characterized by high functionality, high durability and low mass, which translates into economic benefits associated with lower fuel consumption, and the ability of composite materials to be progressively crushed ensures high energy absorption and thus passenger safety. It was proved that considering various types of composite materials investigated by scientists from around the

world (based on glass fibers, aramid fibers and carbon fibers, and more recently also natural fibers and various types of matrix) [1, 2], carbon fiber-reinforced composites in each case are the most efficient as energy absorbing elements and are distinguished by their excellent stiffness to mass ratio [3-9]. However, in order that composite elements could work effectively in real conditions, detailed knowledge of factors affecting the behavior of a composite element absorbing energy and proper guidelines for designing such elements are necessary. Experimental studies carried out over the last decades have shown that apart from the reinforcement and matrix properties, a number of other factors have a significant influence on the capability of stable progressive crushing and on the amount of energy absorbed. They are, among others, element geometry [10, 11], the ratio of wall thickness to diameter t/D [12, 13], loading conditions [14], and element architecture [12]. In addition, it was shown that circular cross-sections absorb more energy (SEA) compared to other cross-section shapes, such as square, rectangular or hexagonal [15-17]. The results of many works have proven that the fiber arrangement (orientation) plays a significant role in the amount of absorbed energy. It was found that fibers with the 0/90 system allow absorption of the largest amounts of energy in comparison with the ±45 system [3, 18, 19]. In addition, in [12] it was pointed out that not only fiber orientation was important, but also the layer distribution and the ratio of the amount of hoop fibers to the amount of axial fibers (H/A, hoop fiber/axial fiber ratio). An increase in the amount of axial fibers results in a significant growth in the force necessary to crush the element, which increases the absorbed energy value. In addition, the important role of the position of the hoop fibers and axial fibers in the energy absorbing element was indicated. At the same H/A value, a symmetrical system was examined where all the hoop fibers were in the center of the wall, and the case where all the hoop fibers were located outside. It was proven that the system in which all the hoop fibers were on the outside and the layers of axial fibers were in the center allowed absorption of the largest amounts of energy. When comparing the symmetrical arrangement of individual layers (fibers of one type grouped in one layer) and the layers of axial and hoop fibers arranged alternately, higher forces were obtained for the symmetrical layer system (hoop fibers in two layers separated by one layer of axial fibers) [12].

Considering the published research results, as well as the fact that there are relatively few publications regarding the H/A factor and the lack of information about the scale effect on the amount of absorbed energy, the aim of this paper is to investigate the influence of the share of axial fibers in the energy absorbing elements on SEA in the process of progressive crushing of composite tubes. The presented research results concern elements in two sizes in order to present the effect of scale on the amount of energy absorbed in this process.

DEFINITIONS

The total amount of energy absorbed E_{tot} is determined by the total area under the load displacement curve for each specimen

$$E_{tot} \int_0^i P dl$$

where: E_{tot} - energy absorbed by the structure, P - crushing force, l - crushing stroke SEA:

$$SEA = \frac{E_{tot}}{\rho A l}$$

where: ρ - mean density of the tube, A - cross-sectional area of the tube, l - crushed stroke.

To determine the influence of the structure architecture on the energy absorption a new coefficient is introduced, $AFMF$ - Axial Fiber Mass Fraction, which determines the mass fraction of axial fibers in relation to the total mass of all the fibers in the specimen

$$AFMF = \frac{M_{axf}}{M_f}$$

where: M_{axf} - mass of axial fibers, M_f - mass of all fibers.

EXPERIMENTAL STUDIES

In the experimental part of this paper two sets of composite samples with internal diameters d_w = 42 mm - Group I and d_w = 20 mm - Group II were made. Two types of prepreg CF/epoxy by Impregnatex Compositi were used. Plain weave (dry areal weight 160 g/m^2) and unidirectional (UD dry areal weight 200 g/m^2) prepregs were used. The first stage was proper winding of the prepreg layers onto a Teflon core of a given diameter, followed by curing in an autoclave at 130°C for about 3 hours. In this way, a set of tubes with a length of 0.5 m was made, which were then cut into samples with a length of 68 mm (in the case of diameter d_w = 42 mm) and 34 mm (in the case of diameter d_w = 20 mm). To ensure stable gradual destruction of the composite tubes, two types of triggering mechanisms are usually used. The first one causes weakness and local stress concentration, causing gradual crushing and lowering of the initial peak of force. Local weakness can be caused by chamfering at various angles, external, internal or bilateral ones [20], by local omission of one layer or two [21], notches [22], tulip shape or other type of weakening [23]. Work [24] investigated the effect of 30°, 45° and 60° chamfering angles on the energy absorption capacity of glass-fiber composite tubes, and determined that a 60° chamfer increases the energy absorption capacity. In work [25] for a carbon-epoxy

composite, a chamfering angle of 70° was used, which resulted in a very small stroke of the initial force in the process. Based on the above test results in this experiment, each sample was finished with a one-sided external 70° chamfer (by grinding). After grinding, the chamfering height on the circumference of the sample was measured and compared. The same dimension of the chamfer on the circumference was a condition for admission of the test sample. The samples were not seasoned. They were stored at a room temperature.

The samples were designed in such a way that they differed from each other by *AFMF* index values. This effect was obtained by using a different number of UD prepreg layers in relation to the number of plain weave prepreg layers, as shown in Figures 1 and 2. Exemplary samples are presented in Figure 3.
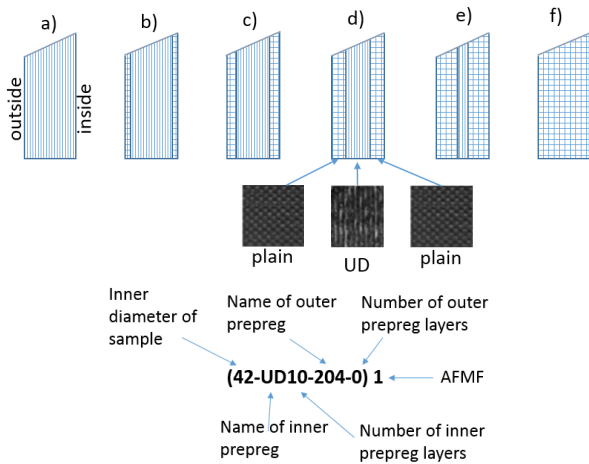
Fig. 1. Wall architecture of samples with inner diameter d_w = 42 mm: a) (42-UD10-160-0)1; b) (42-UD8-160-2)0.9; c) (42-UD6-160-4)0.8; d) (42-UD4-160-6)0.7; e) (42-UD2-160-8)0,6; f) (42-UD0-160-10)0.5 (all ten layers made of plain weave prepreg with dry areal weight 160 g/m²)

Rys. 1. Architektura ścianki dla próbek o średnicy wewnętrznej d_w = = 42 mm: a) (42-UD10-160-0)1; b) (42-UD8-160-2)0.9; c) (42--UD6-160-4)0.8; d) (42-UD4-160-6)0.7; e) (42-UD2-160-8)0,6; f) (42-UD0-160-10)0.5 (wszystkie dziesięć warstw wykonane z preimpregnatu o gramaturze suchej tkaniny 160 g/m²)
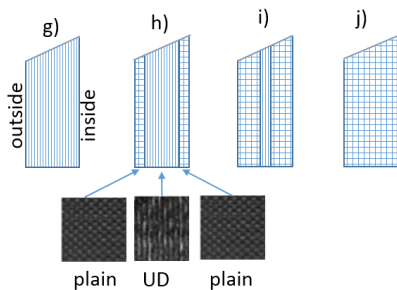
Fig. 2. Architecture of samples with inner diameter d_w = 20 mm: g) (20-UD5-160-0)1 (all five layers made of UD prepreg of dry areal weight 200 g/m²); h) (20-UD3-160-2)0.8; i) (20-UD1-160-4)0,6; j) (20-UD0-160-5)0.5 (all five layers made of plain weave prepreg with dry areal weight 160 g/m²)

Rys. 2. Architektura próbek o średnicy wewnętrznej d_w = 20 mm: g) (20-UD5-160-0)1 (wszystkie pięć warstw wykonane z preimpregnatu o gramaturze suchej tkaniny 200 g/m² UD); h) (20-UD3-160-2)0.8; i) (20-UD1-160-4)0,6; j) (20-UD0-160-5)0.5 (wszystkie pięć warstw wykonane z preimpregnatu o gramaturze suchej tkaniny 160 g/m² splot płócienny)
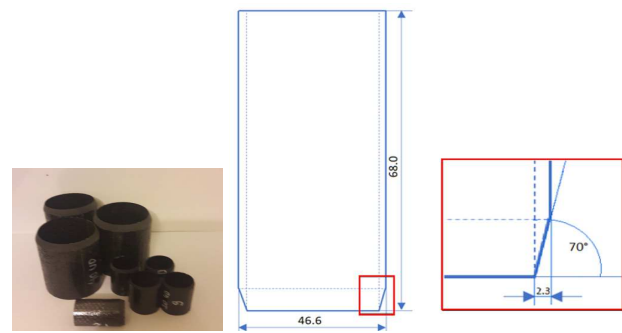
Fig. 3. Examples of samples used for testing (Group I and Group II), chamfering on exemplary sample from Group I

Rys. 3. Przykładowe próbki użyte do badań (grupa I i grupa II), fazowanie na przykładzie próbki z grupy I

EXPERIMENTAL STUDIES IN DYNAMIC CONDITIONS

Tests of energy absorbing elements are usually carried out in two ways: in quasi-static and dynamic conditions. In the quasi-static tests, the energy absorbing element is crushed at a constant velocity, while in the dynamic tests the velocity changes (decreases from the initial value to zero as the energy absorbs through the sample). In other words, in dynamic tests, the velocity is not a constant value as in real conditions. Hence, quasi-static tests may not reflect the true working conditions of such an element. Therefore, the study was carried out under dynamic conditions. Dynamic crushing tests of samples from both groups were carried out at room temperature (22°C) using a drop hammer. In order to ensure stable crushing of the tested samples, apart from chamfering one edge, a second type of triggering mechanism was used, which at the same time was an outer element (plug initiator) in the form of a ring that could be used to generate progressive crushing of the element along its entire length. In works [26, 25], initiators with different radii were applied and it was found that a reduction in the radius led to an increase in forces in the process and thus an increase in SEA, which was also confirmed in [27]. In the present experimental studies the introduced plug initiators were made in two versions (the smaller one weighing 180 g and the bigger one weighing 250 g) for both groups of samples (Fig. 4). In both cases the inner edge was finished with the same radius equal to 1 mm.
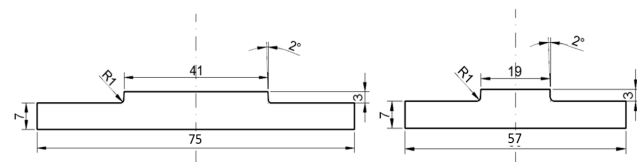
Fig. 4. Plug initiators used in experimental research

Rys. 4. Inicjatory zastosowane w badaniach eksperymentalnych

Three samples were tested for each case. Depending on the configuration of the layers (AFMF), the samples absorbed a different amount of energy in the process,

forcing in some cases adjustment of the height of the fall and the weight of the hammer to the type of sample. The collected data made it possible to obtain information on the specific energy absorption (SEA) but also about the behavior of the tested element during the process (initial force, magnitude of steady state force, obtained displacement).

During the experimental dynamic investigations, a drop tower was used. A diagram of the main elements of the loading system is presented in Figure 5.
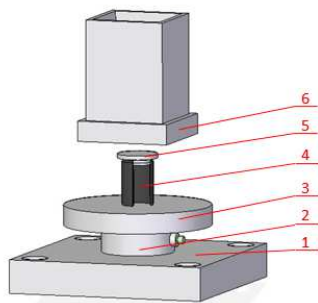
Fig. 5. General view of drop tower loading system: 1 - steel base, 2 - transmitted force transducer, 3 - anvil, 4 - sample (sectional view), 5 - plug initiator, 6 - flat impactor

Rys. 5. Widok systemu obciążania młota opadowego: 1 - podstawa, 2 - przetwornik, 3 - kowadło, 4 - próbka, 5 - inicjator, 6 - młot

A transmitted force transducer 2 (Fig. 5) was mounted on the steel base of the drop tower. A cylindrical anvil 3 was mounted on the transmitted force transducer. Samples 4 equipped with a plug initiator 5 were placed on the anvil 3 and, as a result, the transmitted forces were measured during the drop tests. A PCB Piezotronics impact force transducer model 200C50 was used to measure the transmitted forces. Displacement of the carriage and the impactor was measured with a noncontact laser transducer LK-G502 (Keyence). The velocity of the impactor was measured with two laser gates located at the distance of 50 mm. The signals from the force transducer, displacement transducer and two laser gates were recorded with a computer and an A/D computer board NI USB-6361 (National Instruments, USA). In the set-up, the signals were recorded digitally with a 10 µs sampling step. All the data were processed with a dedicated computer programme.

RESULTS OF EXPERIMENTAL STUDIES

As a result of the tests carried out using the drop hammer, force-displacement dependencies for each type of samples were obtained. The results for representative samples from Group I (diameter d_w = 42 mm) are shown in Figure 6, the view of representative samples after the experiment is shown in Figure 7.

The pictures of the samples from Group I show the different behavior of the energy absorbing element depending on its architecture. The highest forces are observed in the case of the sample containing only axial

fibers. Such an element after the process has a characteristic look. One can see division into so-called "petals" and the effect of strong bending and breaking of axial fibers at the initiator radius. Comparing the force graphs in the displacement function with the appearance of the sample after the experiment, it can be concluded that the least effective architecture from the point of view of energy absorption is the system where the AFMF is 0.5, that is half the fibers are axial fibers and half are hoop fibers. This arrangement also caused strong crushing of the composite during the process.
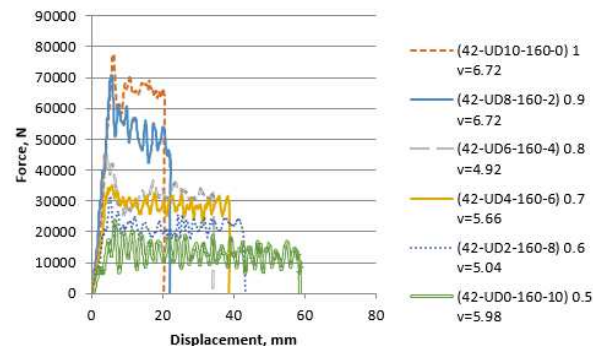
Fig. 6. Relationship between force and displacement for individual geometrical variants of large samples (Group I). Legend contains information about sample designation, AFMF coefficient value and speed in [m/s]

Rys. 6. Zależność między siłą a przemieszczeniem dla poszczególnych wariantów geometrycznych dużych próbek (grupa I). Legenda zawiera informację kolejno o oznaczeniu próbki, wartość współczynnika AFMF oraz prędkość w [m/s]
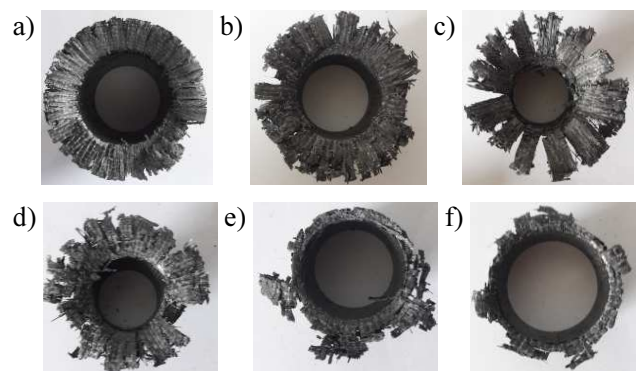
Fig. 7. Example view of samples from Group I (internal diameter d_w = 42 mm) after test: a) AFMF = 1; b) AFMF = 0.9; c) AFMF = 0.8; d) AFMF = 0.7; e) AFMF = 0.6; f) AFMF = 0.5

Rys. 7. Przykładowy widok próbek z grupy I (o średnicy wewnętrznej d_w = 42 mm) po wykonaniu testu: a) AFMF = 1; b) AFMF = 0.9; c) AFMF = 0.8; d) AFMF = 0.7; e) AFMF = 0.6; f) AFMF = 0.5

Based on the obtained force waveforms in the displacement function, SEA calculations for all the variants of the tested samples were made. The results are shown in graphs (Fig. 8).

Similarly for the samples from Group II, the relationships of the force and displacement (Fig. 9) is presented. The view of representative samples after the experiment (Fig. 10) and the calculated SEA for each tested sample (Fig. 11) are also shown.
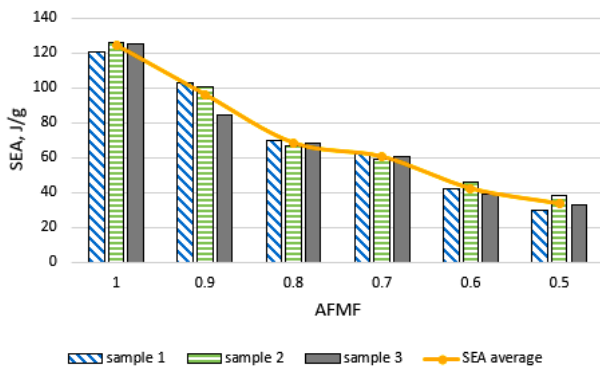
Fig. 8. SEA depending on sample architecture (mass fraction of axial fibers); dynamic test, Group I

Rys. 8. SEA w zależności od architektury próbek (udziału masowego włókien osiowych); test dynamiczny, grupa I
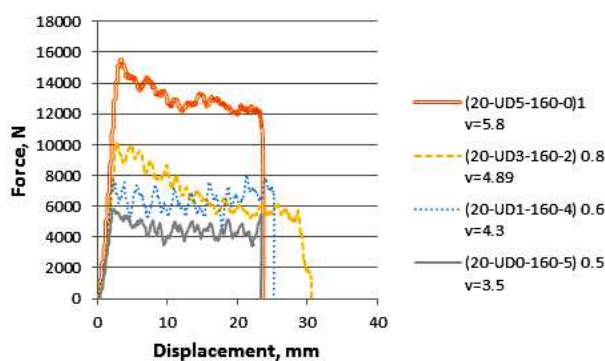
Fig. 9. Relationship between force and displacement for individual geometric variants of small samples (Group II). Legend contains information about sample designation, AFMF coefficient value and speed in [m/s]

Rys. 9. Zależność między siłą a przemieszczeniem dla poszczególnych wariantów geometrycznych próbek małych (grupa II). Legenda zawiera informację kolejno o oznaczeniu próbki, wartość współczynnika AFMF oraz prędkość w [m/s]
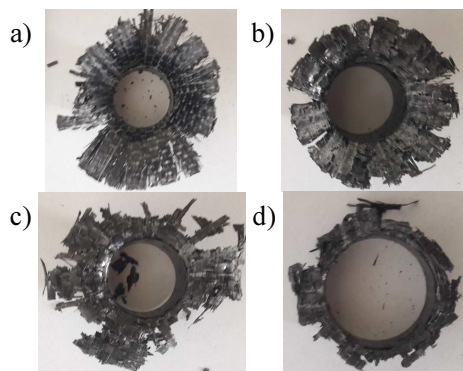
Fig. 10. Example view of samples from Group II (with an inner diameter of d_w = 20 mm) after test: a) AFMF = 1; b) AFMF = 0.8; c) AFMF = 0.6; d) AFMF = 0.5

Rys. 10. Przykładowy widok próbek z grupy II (o średnicy wewnętrznej d_w = 20 mm) po wykonaniu testu: a) AFMF = 1; b) AFMF = 0.8; c) AFMF= 0.6; d) AFMF = 0.5

To illustrate the effect of the scale, a graph of the mean SEA value was made for both groups of samples (Group I and Group II) from the AFMF coefficient value. It should be noted that both groups of samples were designed and made in such a way that despite

the difference in size, common AFMF coefficient values existed and that the tested samples had similar t/d_w parameter values where d_w is the inner diameter and t - the average wall thickness. For the samples from Group I t/d_w = 0.053, and for the samples from Group II t/d_w = 0.057. Thanks to this, it is possible to compare the energy absorption effects in these two cases and to assess the impact of the scale in this type of process. When analyzing the graph (Fig. 12) it can be seen that for large AFMF coefficient values, similar SEA values are obtained. For smaller AFMF values, larger discrepancies in SEA are visible in favor of smaller samples (Group II).
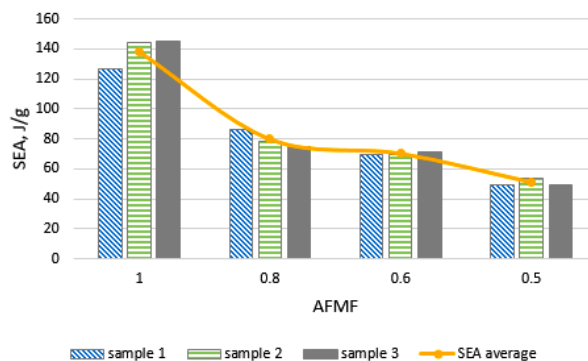
Fig. 11. SEA depending on sample architecture (AFMF); dynamic test, Group II

Rys.11. SEA w zależności od architektury próbek (udziału masowego włókien osiowych AFMF); test dynamiczny, grupa II
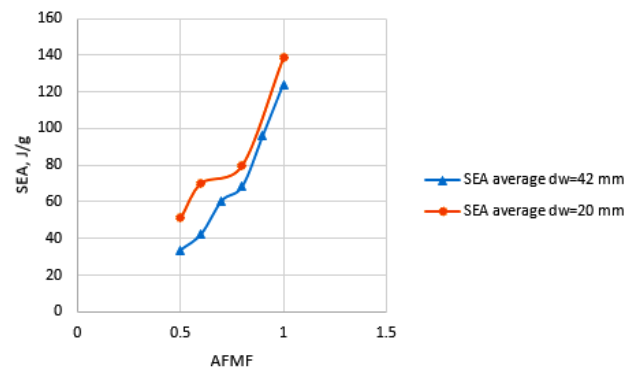
Fig. 12. Comparison of obtained mean SEA values depending on AFMF for two sample sizes (Group I and Group II)

Rys. 12. Porównanie uzyskanych średnich wartości SEA w zależności od udziału włókien osiowych AFMF dla dwóch wielkości próbek (grupa I oraz grupa II)

CONCLUSIONS

The application of a one-sided chamfer on the test samples resulted in the initiation of progressive gradual crushing of the tested energy absorbing elements without a significant peak of force at the beginning of the process. Using an external plug initiator provided stable continuation of the process.

The greatest forces in the process of dynamic progressive crushing of the samples were obtained for the AFMF factor of 1. As the value of this coefficient de-

creases, the magnitude of force decreases for both groups of samples (Group I and Group II). The calculated SEA values indicate that the higher the share of axial fibers, the higher the amount of energy absorbed. For an AFMF equal to 0.5, only 27% of the energy value was obtained compared to the samples for which the AFMF was 1 for the Group I samples and 38% for the Group II samples.

The differences in the amount of energy absorbed in the case of different sample sizes were recorded, which may indicate the occurrence of the phenomenon of scale in this type of processes. The SEA for the Group I and AFMF = 1 samples is 92% of the SEA value for the Group II samples and 63% for AFMF = 0.5, respectively.

REFERENCES

[1] Yan L., Chouwa N., Jayaraman K., On energy absorption capacity, flexural and dynamic properties of flax/epoxy composite tubes, Fibers and Polymers 2014, 15, 1270--1277.

[2] Alkbir M.F.M., Sapuan S.M., Nuraini A.A., Ishak M.R., Fibre properties and crashworthiness parameters of natural fibre-reinforced composite structure: A literature review, Composite Structures 2016, 148, 59-73.

[3] Hull D., A unified approach to progressive crushing of fibre-reinforced composite tubes, Compos. Sci. Technol. 1991, 40, 377-421

[4] Farley GL., Jones R.M., Crushing characteristic of continuous fiber-reinforced composite tubes, J. Compos. Mater. 1992, 26, 37-50.

[5] Thornton P.H., Edward J., Energy absorption in composite tubes, Journal of Composite Materials 1982, 16, 521-545.

[6] Farley G.L., Energy absorption of composite materials, Journal of Composite Materials 1983, 17, 267-279.

[7] Schmueser D.W., Wickliffe L.E., Impact energy absorption of continuous fiber composite tubes, J. Eng. Mat. Trans. ASME 1987, 72, 72-77.

[8] Ramakrishna S., Hamada H., Maekawa Z., Energy absorption behavior of carbon fiber reinforced thermoplastic composite tubes, Journal of Thermoplastic Composite Materials 1995, 14, 1121-1141.

[9] Mamalis A., Manolakos D., Ioannidis M., Papapostolou D., On the experimental investigation of crash energy absorption in laminate splaying collapse mode of FRP tubular components. Compos. Struct. 2005, 70, 413-29.

[10] Alkoles O.M.S., Mahdi E., Hamouda A.M.S., Sahari B.B., Ellipticity ratio effects in the energy absorption of axially crushed composite tubes, Applied Composite Materials 2003, 10, 339-363.

[11] Czaplicki M., Robertson R., Thornton P., Comparison of bevel and tulip triggered pultruded tubes for energy absorption, Composites Science and Technology 1991, 40, 31-46.

[12] Farley G.L., Effect of specimen geometry on the energy absorption capability of composite materials, Journal of Composite Materials 1986, 20, 390-400.

[13] Gupta N., Velmurugan R., Gupta S., An analysis of axial crushing of composite tubes, Journal of Composite Materials 1997, 31, 1262-86.

[14] David M., Johnson A., Voggenreiter H., Analysis of crushing response of composite crashworthy structures, Applied Composite Materials 2013, 20, 773-787.

[15] Thornton P., The crush behavior of pultruded tubes at high strain rates, Journal of Composite Materials 1990, 24, 594--615.

[16] Mamalis A., Manolakos D., Demosthenous G., Ioannidis M., Analysis of failure mechanisms observed in axial collapse of thin-walled circular fiberglass composite tubes, Thin-Walled Structures 1996, 24, 335-352.

[17] Mamalis A.G., Robinson M., Manolakos D.E., Demosthenous G.A., Ioannidis M., Carruthers J., Crashworthy capability of composite material structures, Composite Structures 1997, 37, 109-134

[18] Pickett L., Dayal V., Effect of tube geometry and ply-angle on energy absorption of a circular glass/epoxy crush tube - a numerical study, Compos. Part B: Eng. 2012, 43, 2960-2967.

[19] Thornton, P.H., Energy absorption in composite structures, J. Comp. Mats 1979, 13, 247-262.

[20] Song H., Zhao X., Energy absorption behavior of double-chamfer triggered glass/epoxy circular tubes, Journal of Composite Materials 2002, 36, 2183-2201.

[21] Joosten M.W., Dutton S., Kelly D., Thomson R., Experimental evaluation of the crush energy absorption of triggered composite sandwich panels under quasi-static edgewise compressive loading, Composites Part A 2010, 41, 1099-1106.

[22] Yan L., Chouwa N., Jayaraman K., Effect of triggering and polyurethane foam-filler on axial crushing of natural flax/epoxy composite tubes, Materials & Design 2014, 56, 528-541.

[23] Mamalis A.G., Manolakos D.E., Ioannidis M.B., Papapostolou D.P., The static and dynamic axial collapse of CFRP square composite tubes: finite element modelling, Composite Structures 2006, 74, 213-25.

[24] Jiménez M.A., Miravete A, Larrodé E., Revuelta D., Effect of trigger geometry on energy absorption in composite profiles, Composite Structures 2000, 48, 107-111.

[25] Hou T., Pearce G.M.K., Prusty B.G., Kelly D.W., Thomson R.S., Pressurized composite tubes as variable load energy absorbers, Composite Structures 2015, 120, 346-357.

[26] Siromani D., Henderson G., Mikita D., Mirarchi K., Park R., Smolko J., Awerbuch J., Tan Tein-Min, An experimental study on the effect of failure trigger mechanisms on the energy absorption capability of CFRP tubes under axial compression, Composites: Part A 2014, 64, 25-35.

[27] Atthapreyangkul A., Gangadhara Prusty B., Experimental and numerical analysis on the geometrical parameters towards the maximum SEA of CFRP components, Composite Structures 2017, 164, 229-236.